ISSN 1995-0780, Nanotechnologies in Russia, 2019, Vol. 14, Nos. 9–10, pp. 497–503. © Pleiades Publishing, Ltd., 2019.
Russian Text © The Author(s), 2019, published in Rossiiskie Nanotekhnologii, 2019, Vol. 14, Nos. 9–10.

NANOBIOLOGY AND GENETICS, OMICS

Studying and Assessing the Toxicity of Calcium Oxide Nanoparticles under One-Time Inhalation Exposure

N. V. Zaitseva[a], M. A. Zemlyanova[a,b,c,*], M. S. Stepankov[a,b], and A. M. Ignatova[a,c]

[a] *Federal Scientific Center for Medical and Preventive Health Risk Management Technologies, Perm, Russia*
[b] *Perm State National Research University, Perm, Russia*
[c] *Perm National Research Polytechnic University, Perm, Russia*
**e-mail: zem@fcrisk.ru*

Received February 3, 2020; revised February 3, 2020; accepted February 13, 2020

Abstract—Under a single 4 hour inhalation exposure to aerosol containing an aqueous suspension of calcium oxide nanoparticles (CaO) in an actual concentration of 6.68 mg/m^3, the accumulation of calcium increased in the lungs (by 1.52 times), in the brain (by 1.55 times) and in the liver (by 1.25 times) relative to the control, while exposure to a microdispersed analog in a concentration of 6.37 mg/m^3 resulted in an increase in the indicator only in the brain (by 1.27 times). At the same time, the calcium concentration in the brain of animals in the experimental group is higher than in the comparison group (by 1.22 times). After exposure to CaO nano- and microparticles a subarachnoid hemorrhage in the brain tissues was found. The development of pathomorphological changes in the form of lymphoid tissue hyperplasia, eosinophilia, acute arterial plethora, and hemorrhagic lung infarcts, as well as the hydropic and hyaline-drop dystrophy of parenchymal liver tissue was observed only after exposure to CaO nanoparticles. The identified features of the bioaccumulation and pathomorphological changes under inhalation exposure to CaO nanoparticles demonstrate that the studied nanomaterial has a higher level of toxicity in comparison to its microdispersed analog.

DOI: 10.1134/S1995078019050148

INTRODUCTION

The widespread introduction of nanomaterials is expected to have a significant impact in different fields of human economic activities, which will lead to improvement and even revolutionary changes in many technologies and industries [1]. These prediction are associated with the unique physical and chemical properties of nanomaterials due to their small size, high surface area, shape, surface charge, etc. At the same time, the inherent properties of nanomaterials determine their high penetrating ability, which can result in an increase in their toxic properties when they enter the human body at all stages of production and consumption of products [2].

Calcium oxide nanoparticles (CaO) are among these materials. Due to their antibacterial properties, they are used in medicine as a part of antibacterial drugs, in the food industry as a component of food packaging, and in water purification processes [3–5]. As well, CaO nanoparticles are used as components in fire-retardant materials, bio-fuel systems, and in cleaning territories from contamination with chemical weapons components [5, 6].

It is known that the damaging effect of CaO nanoparticles on organs and tissues is manifested when they are ingested orally [7], which indicates their ability to penetrate the epithelial barrier of the gastrointestinal tract. In addition, it is possible that CaO nanoparticles can overcome the hematoencephalic barrier [8]. There are data on the ability of the studied nanoparticles to produce reactive oxygen species (ROS) [9], which can further destroy the cell wall of bacteria by reacting with the carbonyl group in the peptide bonds of polyunsaturated phospholipids, which are one of the components in any cell wall [9]. CaO nanoparticles destroy cell membranes via interaction with the amide structures of the proteins included in their composition [9]. Subcutaneous introduction of the studied nanomaterial into rats for 3 months led to degeneration and necrosis of liver and kidney tissues and hemorrhages in the kidneys and brain [8]. The toxicity of CaO nanoparticles for the aquatic organisms Cyprinus carpio and Danio rerio was revealed: the concentration at which 50% of species in the exposed groups died (LC_{50}) was 235 and 260 mg/dm^3, respectively, and 100% of the species died at 280 and 400 mg/dm^3, respectively [10, 11].

Due to the wide range of applications in various industries, the toxic properties of CaO nanoparticles, as well as a lack of information about their inhalation toxicity, it is particularly relevant to perform research

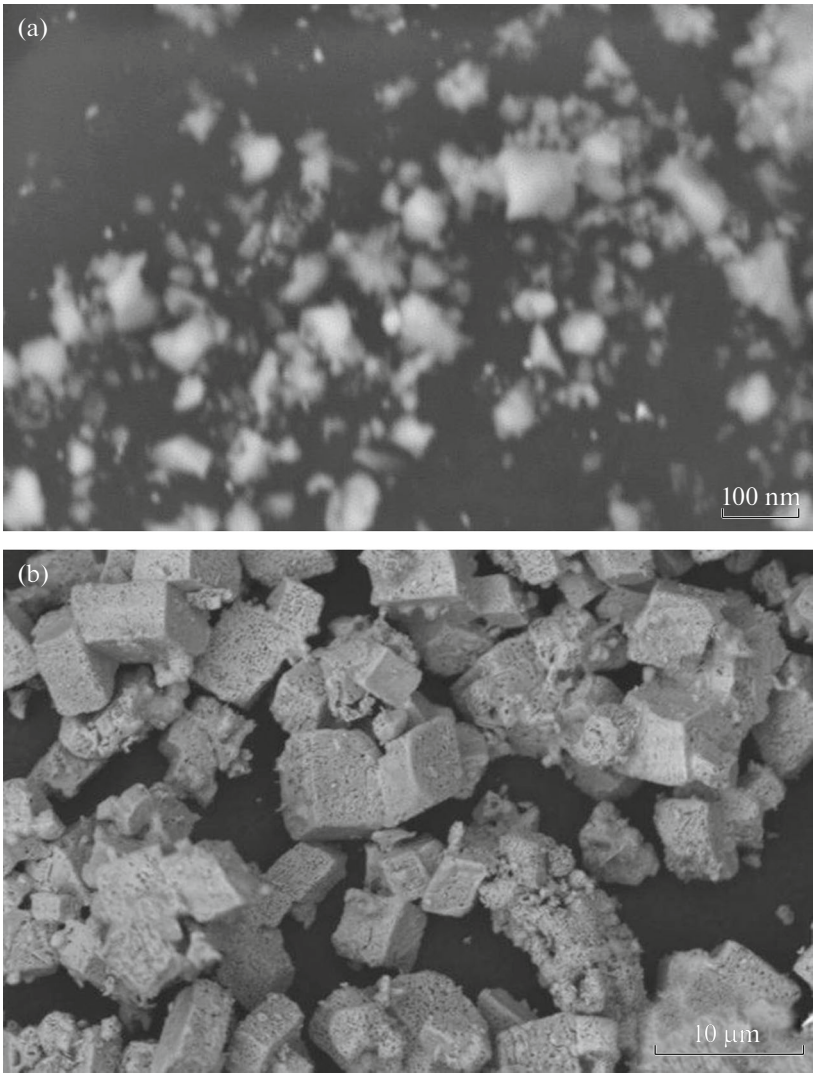

Fig. 1. An REM image of (a) CaO nanoparticles and (b) microparticles.

aimed at compiling the toxicological and hygienic characteristics of this nanomaterial when it enters the body via inhalation.

MATERIALS AND METHODS

Nanodispersed CaO powder (Calcium oxide, CAS 1305-78-8, no. NG04SO1704) produced by Nanografi (Turkey) was used as a test sample. For comparative analysis, a microdispersed CaO powder (Calcium oxide, CAS 1305-78-8, no. 229539) produced by Sigma Aldrich (United States) was used.

The CaO particle size was estimated with scanning electron microscopy (SEM) on a high-resolution s-3400N scanning microscope (HITACHI, Japan).The particle shape and surface properties were determined by image analysis with the universal ImageJ-FiJi software.

The experiment was performed on mature male Wistar rats weighing 250–300 g in accordance with GOST 32646-2014, the requirements of the Ethical committee of the Federal Scientific Center for Medical and Preventive Health Risk Management Technologies and the Guidelines for the care and use of laboratory animals [12]. Experimental animals (n = 36) were randomly assigned to an experimental group (n = 12), a comparison group (n = 12), and a control group (n = 12). Experimental group animals were subjected to one-time 4-hour inhalation exposure to aerosol containing an aqueous suspension of nanodispersed CaO, comparison group animals were exposed under the same conditions to a spray containing an aqueous suspension of microdispersed CaO. Animals were exposed to aerosols in an inhalation system with integrated software using a chamber for the whole body (TSE Systems GmbH, Germany). To generate aerosols, aqueous suspensions of nano-sized CaO and

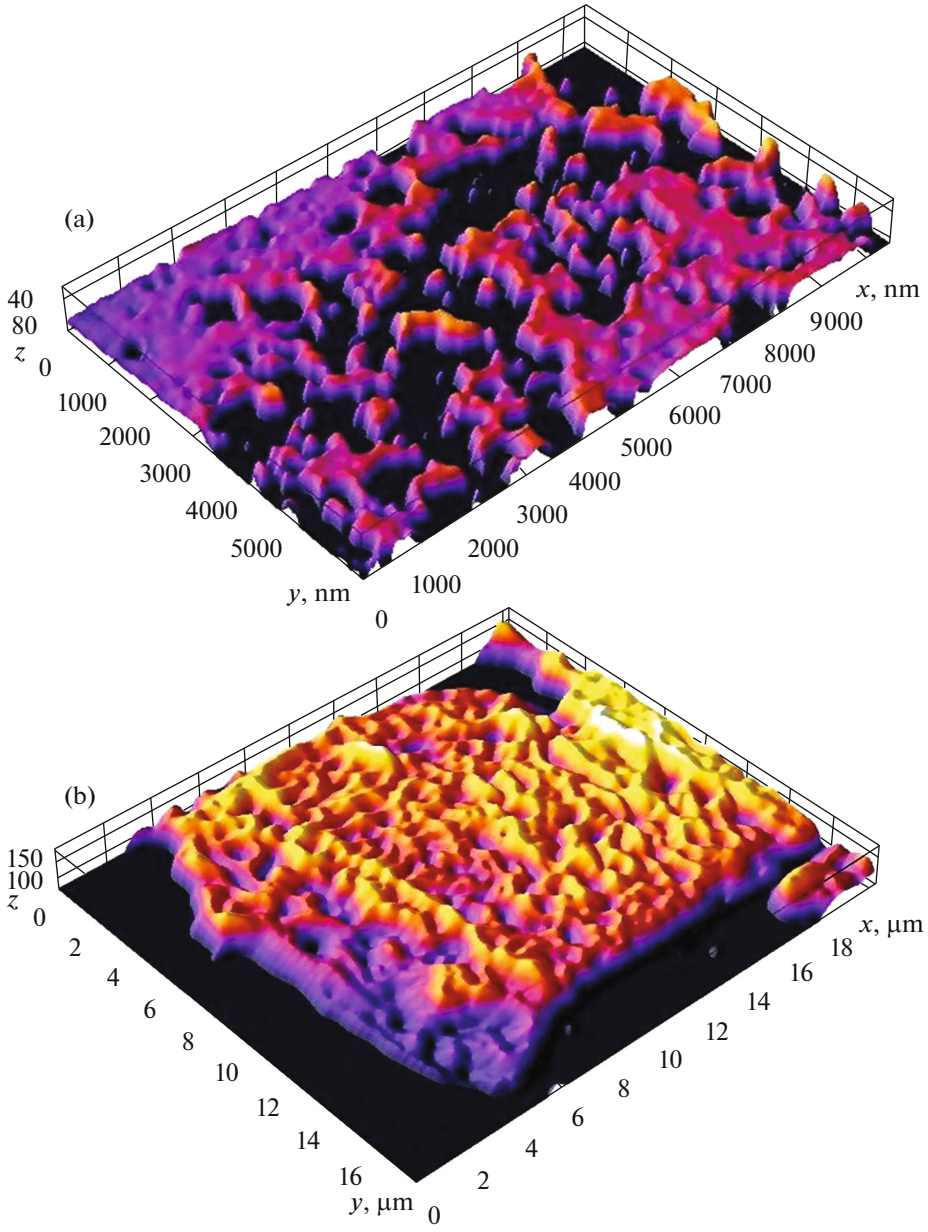

Fig. 2. (Color online) An isometric three-dimensional reconstruction of the surface of (a) CaO nanoparticles and (b) microparticles .

its microdispersed analogue at a concentration of 125 mg/cm^3 were used. Control group animals were kept in similar conditions for the period of the experiment; however, they were not exposed to inhalation of these substances. The animals were not fed during the exposure period. After the inhalation exposure, the observation period for animals was 14 days to determine the possible delayed toxicity of a substance. The characteristics of the air flow in the chamber were as follows: the air inflow was 10 dm^3/min (oxygen concentration of at least 19%, carbon dioxide at least 1%); the feed rate of aqueous suspensions of nano- and microdispersed CaO was 0.4 cm^3/min; air outflow was 10 dm^3/min; pressure fluctuations inside the chamber were equal to 0.4 mbar; the temperature in the chamber was 22–25°C throughout the experiment. Air sampling from the chamber to determine the concentration of the tested substances was carried out on an AFA-KhP-10-1 filter throughout the entire exposure time with a feed rate of 2 dm^3/min. The actual concentration of nanosized CaO in the air of the inhalation chamber was 6.68 mg/m^3; that of the microdispersed CaO was 6.37 mg/m^3.

At the end of the observation period the animals were removed from the experiment via cervical dislocation. To study the calcium bioaccumulation, the

Table 1. Calcium bioaccumulation in the organs of Wistar rats after one-time inhalation exposure to an aerosol containing an aqueous suspension of nano-and microdispersed calcium oxide ($p \le 0.05$)

Animal group	Indicator		Calcium concentration in the organ, mmol/dm^3				
			lungs	kidneys	brain	liver	blood
Control group	Mean value ($M \pm m$)		2.02 ± 0.31	1.00 ± 0.19	1.46 ± 0.33	3.59 ± 0.41	0.18 ± 0.03
Comparison group	Mean value ($M \pm m$)		2.02 ± 0.55	0.86 ± 0.10	1.86 ± 0.14	3.39 ± 0.30	0.19 ± 0.04
	Intergroup difference with control (p)		0.998	0.141	**0.021**	0.285	0.553
	Multiplicity of differences with control	lower	1.00	1.17	–	1.06	–
		higher	–	–	1.27	–	1.07
Experiment group	Mean value($M \pm m$)		3.07 ± 0.48	1.05 ± 0.21	2.26 ± 0.23	4.47 ± 0.18	0.17 ± 0.03
	Intergroup difference with control (p)		**0.001**	0.686	**0.0004**	**0.001**	0.575
	Multiplicity of differences with control	lower	–	–	–	–	1.05
		higher	1.52	1.05	1.55	1.25	–
	Intergroup difference with comparison group (p)		**0.004**	0.064	**0.002**	**<0.0001**	0.359
	Multiplicity of differences with a comparison group	lower	–	–	–	–	1.13
		higher	1.52	1.22	1.22	1.32	–

lungs, liver, kidneys, brain, and blood were extracted from six animals from each group. The samples were subjected to thermal ashing in a muffle furnace for 9 h at a temperature of 450–500°C. Quantitative determination of the calcium content in the samples was carried out by photometry with the Arsenazo III indicator reagent using a Konelab 20 biochemical automatic analyzer (ThermoFisher, Finland) at a wavelength of 650 (640–670) nm.

A histological study of the lungs, liver, kidneys and brain was performed in six animals of each experimental group. The extracted organs were fixed in a 10% solution of buffered neutral formalin. Dehydration of fixed tissue pieces was performed in an Excelsior ES automatic histological processor (Thermo Scientific, Germany). Histological preparations were made from paraffin sections 3-4 microns thick, staining with hematoxylin and eosin according to a conventional technique in a Varistain Gemini ES staining robot (Thermo Scientific, Germany). Micrographs were made using a Mikroskopkamera AxioCam ERc 5s camera (Carl Zeiss, Germany).

The study results were mathematically processed using parametric statistical methods, preliminary evaluation of whether the results agreed with the normal distribution law, calculation of the sample mean (M) and standard error (m), and testing the hypothesis of matching sample means using the Student's t-test. Differences in the results were considered statistically significant at $p \le 0.05$.

RESULTS AND DISCUSSION

According to the SEM results, the average particle size of the native CaO nanopowder was 343.10 ± 10.15 nm, which is 19.24 times smaller than this parameter for micropowder particles (6600 ± 600 nm) (Fig. 1). At the same time, a large proportion of nanopowder particles (more than 55%) had a size of up to 100 nm. When analyzing images obtained by the REM method, we found that the coefficient of roundness (sphericity) of CaO nanoparticles of up to 100 nm was 0.92 ± 0.03, which significantly differed from this indicator for particles larger than 100 nm (0.77 ± 0.04) that are part of the nanopowder ($p < 0.0001$). The shape of particles of up to 100 nm was close to spherical. The sphericity coefficient of CaO microparticles was 0.79 ± 0.08, which was significantly lower by 1.17 times ($p = 0.003$) than this indicator for nanoparticles. The shape of microparticles was close to cubic. During the three-dimensional reconstruction of CaO nanoparticles, it was found that their surface did not contain significant changes in its structure, which allowed us to consider them as being smooth (Fig. 2). The surface of the particles of the microdispersed analog is rough with an average roughness of 0.15 ± 0.07 μm (Fig. 2).

When studying the bioaccumulation of the tested substances, it was found that after a one-time inhalation exposure to nanodispersed CaO for 4 hours, the concentration of calcium increased in the lungs, brain, and liver of experimental animals by 1.52 ($p = 0.001$), 1.55 ($p = 0.0004$) and 1.25 times ($p = 0.001$), respectively, in comparison with the values of this indicator in control group animals. Similar changes were observed when comparing the experimental and comparison groups: the concentration of calcium in the lungs, brain, and liver after exposure to nanodispersed CaO was higher than when exposed to a microdispersed analog in 1.52 ($p = 0.004$), 1.22 ($p = 0.020$) and

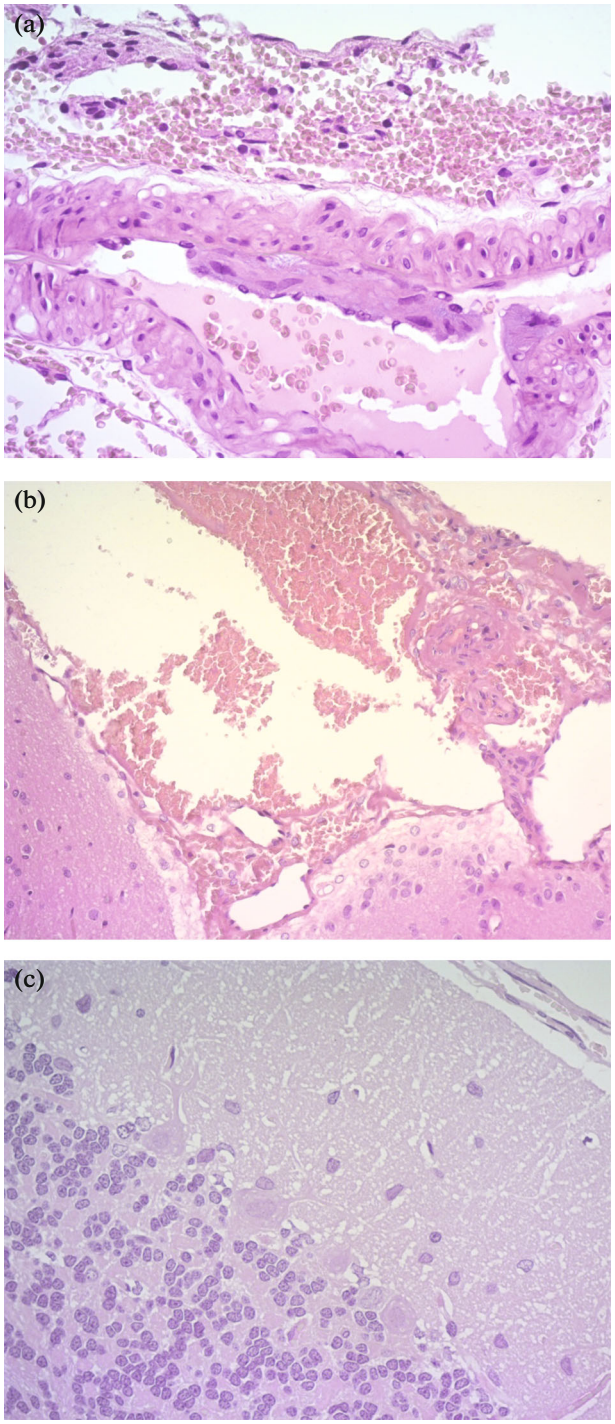

Fig. 3. (Color online) Micrographs of histological preparations of Wistar rats brain tissues (hematoxylin–eosin staining, scale 400 : 1): (a) experimental group; (b) comparison group; (c) control group.

1.32 times ($p < 0.0001$), respectively. In animals exposed to CaO microparticles, the concentration of calcium relative to control increased only in the brain by 1.27 times ($p = 0.021$) (Table 1).

Comparative assessment of pathomorphological changes in the studied organ tissues made it possible to establish similar changes in the brain in the form of a subarachnoid hemorrhage not recorded in animals from the control group in comparison with animals of the experimental and comparison groups (Fig. 3). We observed hyperplasia of lymphoid tissue associated with the wall of the bronchi and blood vessels, eosinophilia, acute plethora, hemorrhagic heart attacks in lung tissues (Fig. 4), and severe hydropic and hyaline droplet dystrophy in parenchymal tissue of the liver in animals exposed to CaO nanoparticles, in contrast to the comparison and control groups (Fig. 5).

The studied CaO sample is a nanomaterial since more than 55% of the particles included in the powder belong to the nanoscale fraction. The established parameters of the size, shape, and surface character of the nanoparticles confirm their high degree of penetration and, therefore, suggest a more pronounced toxicity relative to the micro-sized analog. According to the results of the bioaccumulation study, it was found that during the inhalation, nano- and microparticles of CaO accumulate in the brain, while the degree of accumulation is more pronounced in the nanomaterial, which, unlike the micromaterial, also accumulates in the lungs and liver. A pathomorphological change in the form of subarachnoid hemorrhage was found in the brain of animals of both exposed groups, which coincides with the results obtained earlier [8]. One of the mechanisms of subarachnoid hemorrhage may be related to the accumulation of calcium in the arteries [13]; however, in the presented experiment, the presence of calcium in the brain vessels was not established by histological research methods. The reason for the development of subarachnoid hemorrhage in this case is probably associated with a possible violation of the functions performed by tight contacts [14] and/or pericytes [15] in the blood–brain barrier. A more in-depth study is required to determine the exact mechanism of effects produced by CaO nanoparticles on the brain. Acute hyperemia and hemorrhagic infarcts recorded in the lung tissues of the experimental group of animals indicate a violation of blood circulation. In addition, the lymphoid tissue of the lungs of the animals in the experimental group was subject to hyperplasia, which probably developed during the inflammatory process caused by the action of ROS [16, 17] produced by CaO nanoparticles. ROS generation may be the basis of the mechanism of dystrophic changes established in the liver parenchymal tissue. ROS inhibit the action of sodium–potassium adenosine triphosphatase [18], while Ca^{2+} ions entering the cell displace K^{+} ions. An excess of Ca^{2+} ions in the cytosol activates the calcium pump, with which the cell attempts to eliminate the excess Ca^{2+} through the endoplasmic network [19], where water and ions accumulate, leading to the expansion of the tubules and cisterns of this organelle, which, in turn, causes hydropic dystrophy [20]. Developing hyaline-drop dystrophy of hepatocytes is proba-

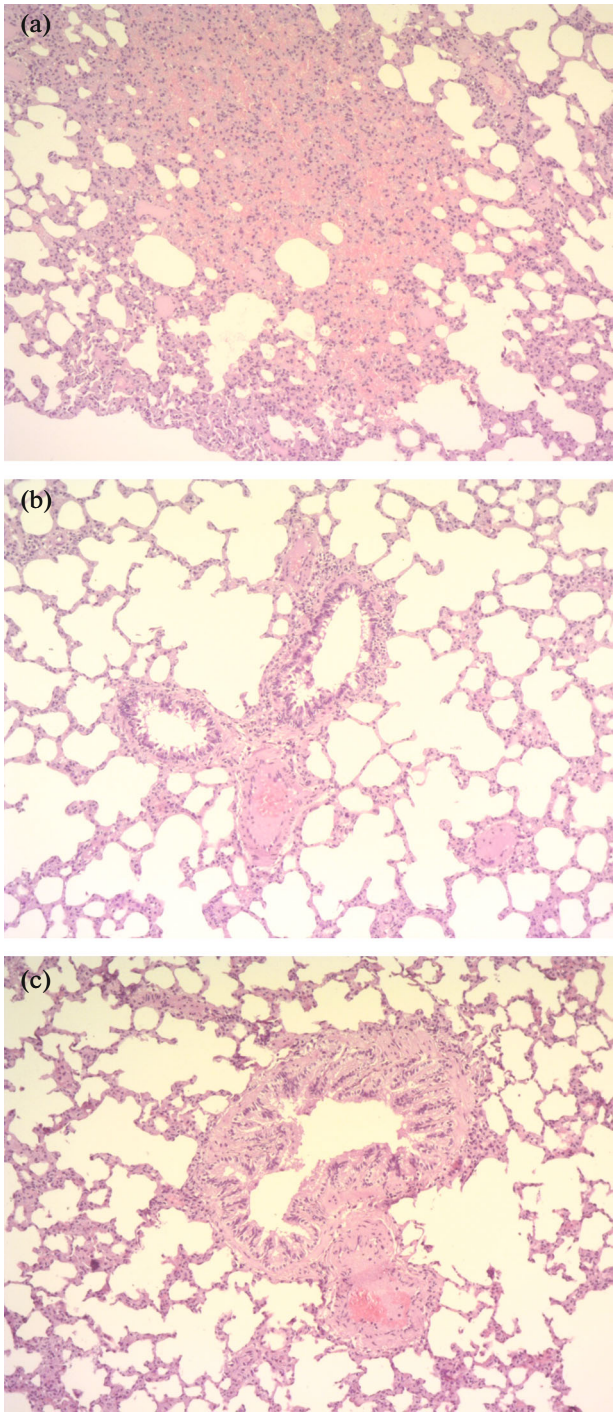

Fig. 4. (Color online) Micrographs of histological preparations of Wistar rats lung tissues (hematoxylin–eosin staining, scale 100 : 1): (a) experimental group; (b) comparison group; (c) control group.

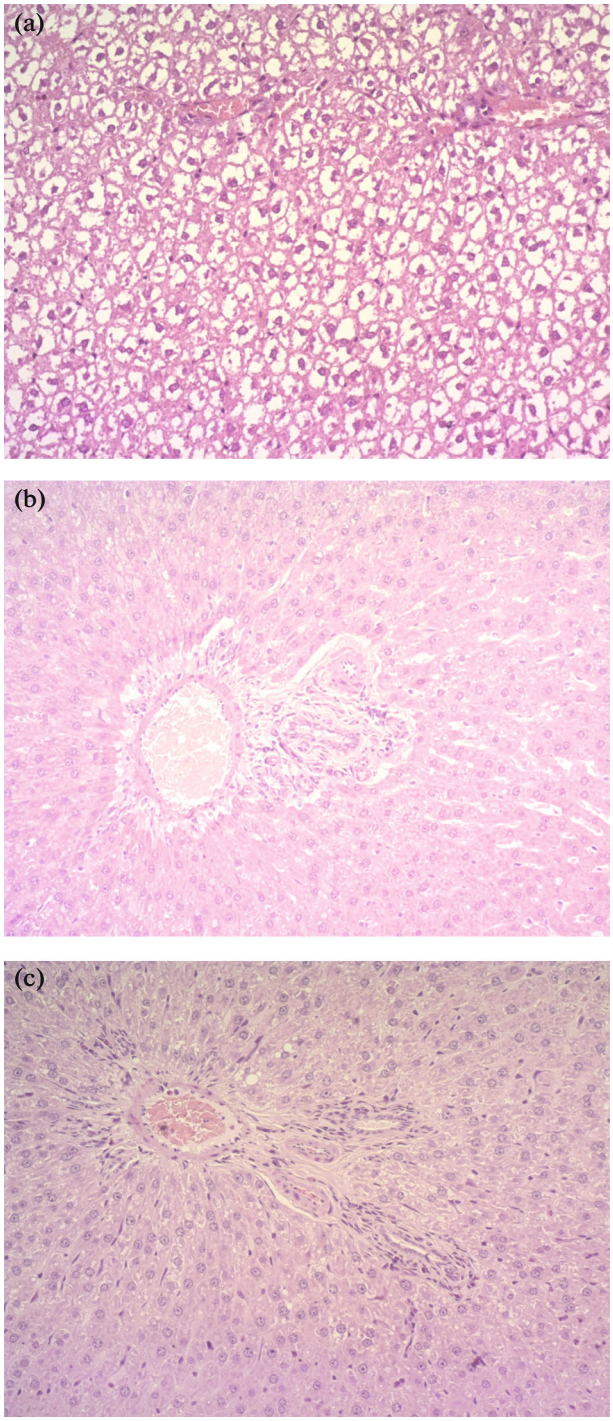

Fig. 5. (Color online) Micrographs of histological preparations of Wistar rats liver tissues (hematoxylin–eosin staining, scale 200 : 1): (a) experimental group; (b) comparison group, (c) control group.

bly a manifestation of perverted protein synthesis, which may indicate the inflammatory response development in the liver parenchyma [20] to the production of ROS. Pathomorphological changes have been found in the liver parenchymal tissue in the form of hepatocyte degeneration after exposure to CaO nanoparticles [8], which is consistent with the results obtained in this study, as well as necrosis, the development of which is natural for dystrophies and, in this case, is most likely due to a longer exposure period.

CONCLUSIONS

As a result of these studies, it was found that Cao nanoparticles under a one-time inhalation exposure had a more pronounced accumulation in comparison with the microdispersed analog; they accumulated in the brain, lungs, and liver of Wistar rats. The action of CaO nano- and microparticles caused comparable pathomorphological changes in the brain tissue; however, the nanomaterial had a greater degree of toxicity, which is manifested via changes in lung and liver tissues that were not established under exposure to micro-sized CaO. It is necessary to consider this result in order to increase the effectiveness of preventive measures for working people and populations who are exposed to CaO nanoparticles, which are inhaled during production and consumption of products.

REFERENCES

1. Benefits and Applications, National Nanotechnology Initiative. http://www.nano.gov/you/nanotechnology-benefits. Accessed January 21, 2020.
2. A. Sukhanova, S. Bozrova, P. Sokolov, et al., "Dependence of nanoparticle toxicity on their physical and chemical properties," Nanoscale Res. Lett. **13** (44), 21 (2018). https://doi.org/10.1186/s11671-018-2457-x
3. S. Abraham and V. P. Saranthy, "Biomedical applications of calcium oxide nanoparticles - a spectroscopic study," Int. J. Pharm. Sci. Rev. Res. **49**, 121 (2018).
4. C. Batt and M. Tortorello, *Encyclopedia of Food Microbiology,* 2nd ed. (Academic, Elsevier, San Diego, 2014).
5. Calcium Oxide (CaO) Nanoparticles – Properties, Applications, AZoNano. 2013. http://www.azonano.com/article.aspx?ArticleID=3365. Accessed January 21, 2020.
6. H. Bai, X. Shen, X. Liu, et al., "Synthesis of porous CaO microsphere and its application in catalyzing transesterification reaction for biodiesel," Trans. Nonferr. Met. **19**, 674 (2009). https://doi.org/10.1016/S1003-6326(10)60130-6
7. S. Al-Shaibani, "The effect of calcium oxide-nanoparticles on the function of the kidney organ in the rats," J. Eng. Appl. Sci. **13**, 7689 (2018).
8. A. R. Butt, S. Ejaz, J. C. Baron, et al., "CaO nanoparticles as a potential drug delivery agent for biomedical applications," Digest J. Nanomater. Biostruct. **10**, 799 (2015).
9. G. Gedda, S. Pandy, Y.-C. Lin, et al., "Antibacterial effect of calcium oxide nano-plates fabricated from shrimp shells," Green Chem. **17**, 3276 (2015). https://doi.org/10.1039/C5GC00615E
10. C. Bhavya, K. Yogendra, K. M. Mahadevan, et al., "Synthesis of calcium oxide nanoparticles and its mortality study on fresh water fish cyprinus carpio," IOSR J. Environ. Sci., Toxicol. Food Technol. **10** (12), 55 (2016).
11. J. Kovrižnych, R. Sotnikova, D. Zeljenkova, et al., "Acute toxicity of 31 different nanoparticles to zebrafish (Danio rerio) tested in adulthood and in early life stages - comparative study," Interdiscipl. Toxicol. **6** (2), 67 (2013). https://doi.org/10.2478/intox-2013-0012
12. Natl. Res. Council of the National Acad., *Guide for the Care and Use of Laboratory Animals* (Natl. Acad. Press, Washington, DC, 2011).
13. S. J. Goldstein, J. G. Sacks, C. Lee, et al., "Computed tomographic findings in cerebral arterial ectasia," Am. J. Neuroradiol., No. 4, 501 (1983).
14. Kim Jung Hun, Kim Jin Hyoung, J. A. Park, S. W. Lee, et al., "Blood-neural barrier: intercellular communication at glio-vascular interface," J. Biochem. Mol. Biol. **39**, 339 (2006). https://doi.org/10.5483/bmbrep.2006.39.4.339
15. S. Liu, D. Agalliu, C. Yu, and M. Fisher, "The role of pericytes in blood-brain barrier function and stroke," Curr. Pharm. Des. **18**, 3653 (2012). https://doi.org/10.2174/138161212802002706
16. C. Pease, T. Rucker, and T. Birk, "Review of the evidence from epidemiology, toxicology and lung bioavailability on the carcinogenicity of inhaled iron oxide particulates," Chem. Res. Toxicol. **29**, 237 (2016). https://doi.org/10.1021/acs.chemrestox.5b00448
17. B. N. Lambrecht and H. Hammad, "The immunology of asthma," Nat. Immunol. **16**, 45 (2015). https://doi.org/10.1038/ni.3049
18. I. Petrushanko, N. Bogdanov, E. Bulygina, et al., "Na-K-ATPase in rat cerebellar granule cells is redox sensitive," Am. J. Physiol., Regul. Integr. Compar. Physiol. **290**, R916 (2006). https://doi.org/10.1152/ajpregu.00038.2005
19. *Medical Biophysics: A textbook for Higher School,* 3rd ed., Ed. by V. Samoilov (SpetsLit, St. Petersburg, 2013) [in Russian].
20. *Pathological Anatomy: Textbook,* 5th ed., Ed. by A. I. Strukov and V. V. Serov (Litterra, Moscow, 2010) [in Russian].